Desalination and Water Treatment
www.deswater.com
doi: 10.5004/dwt.2020.25957

197 (2020) 121–130
September

Study of the stable and metastable phase equilibrium of a ternary system ($NaCl + Na_2SO_4 + H_2O$) in coal-to-liquids wastewater at 323.15 K

Li Zhu, Yu-Long Ma*, Shao-Ying Ge, Di Wu, Cheng Che, Er Liu, Kang-He Zhao

State Key Laboratory of High-efficiency Utilization of Coal and Green Chemical Engineering, College of Chemistry and Chemical Engineering, Ningxia University, Helanshan Rd. 539, Yinchuan 750021, China, Tel. +86 951 2062859; Fax: +86 951 2062859; emails: yulongma796@sohu.com (Y.-L. Ma), 614029492@qq.com (L. Zhu), 53655569@qq.com (S.-Y. Ge), 1499701251@qq.com (D. Wu), 1466325224@qq.com (C. Che), 2942171186@qq.com (E. Liu), 285866286@qq.com (K.-H. Zhao)

Received 26 August 2019; Accepted 11 April 2020

ABSTRACT

The stable and metastable phase equilibria of the ternary system ($NaCl + Na_2SO_4 + H_2O$) in coal-to-liquids wastewater were studied at 323.15 K. The solubility of the stable and metastable phase equilibria were investigated by the isothermal solution saturation and isothermal evaporation methods, respectively. According to the experimental results, stable, and metastable phase diagrams were plotted. For the stable phase diagrams in coal-to-liquids wastewater and in pure water, no significant solubility difference on the NaCl-rich side of the ternary system was found. However, the solubility on the Na_2SO_4-rich side in coal-to-liquids wastewater was lower than that in pure water. The same result was also shown in the metastable phase diagram, but the co-nucleation point moved significantly to the left in the metastable phase diagram. When comparing the ternary system in coal-to-liquids wastewater and pure water, it was found that the average metastable zone width increased by approximately 76.89% in coal-to-liquids wastewater. These experimental results revealed that the stable and metastable phase equilibria for the ternary system ($NaCl + Na_2SO_4 + H_2O$) were significantly affected by the presence of organic impurities in coal-to-liquids wastewater. The experimental data can provide a basis for the desalination process of coal-to-liquids wastewater.

Keywords: Stable phase diagrams; Metastable phase diagrams; Organic impurity; Coal-to-liquids wastewater

1. Introduction

Water shortage is a major problem facing the world [1,2]. Water reuse has become a new way to solve this problem. Recently, the focus of water recycling has been on how to recycle and treat sewage. The high salinity wastewater discharged from energy and textile industries [3], paper mills [4], leather processing [5], food engineering and other processes has become a difficult point in wastewater treatment, which seriously limits the development of these industries. This is especially true of the coal chemical industry, which contributes various inorganic salts and organic pollutants to wastewater [6,7]. Currently, with the rapid development of coal chemical enterprises, the key field of coal-to-liquids wastewater treatment has shifted from wastewater treatment to a crystallization process.

Coal-to-liquids wastewater is the final discharge of wastewater from a coal-to-liquids production process [8–10]. Coal-to-liquids wastewater has a complex composition and high chemical oxygen demand. Generally, most coal-to-liquids wastewater is recovered after membrane concentration, and the remaining wastewater is sent to a desalination system. The remaining wastewater contains many inorganic ions, such as Na^+, Cl^-, NO_3^-, and SO_4^{2-}. By

* Corresponding author.

using evaporation crystallization technology, the purpose of brine separation has been achieved. However, the crystalline salt obtained by evaporation crystallization has low quality and high impurity salt content, so it can only be treated as hazardous waste [11,12]. This is not only harmful to the environment but also a waste of resources. Therefore, it is highly crucial to study the separation and crystallization of inorganic salts and increase the recycling utilization rate of inorganic salts from coal-to-liquids wastewater [13]. Phase equilibrium of a water-salt system can provide theoretical guidance in the process of salt extraction.

It is well known that coal-to-liquids wastewater has a typical inorganic composition of NaCl + Na_2SO_4 + H_2O. To separate NaCl and Na_2SO_4 from the solution, it is essential and necessary to understand the phase diagram and physical properties of the system. In other words, the determination of phase diagrams has both theoretical and experimental value. Zhang et al. [14], Bian et al. [15], and other experts [16] studied the liquid–solid equilibrium of a ternary system $Na^+//Cl^-$, SO_4^{2-}–H_2O at 268.15–373.15 K, and carried out a detailed analysis. In the study of Su et al. [17], the effect of phenol on the solubility of Na_2SO_4 was investigated. It was found that the presence of phenol could inhibit the solubility of Na_2SO_4 in water. This result shows that the phase equilibrium of a water-salt system will change greatly in the presence of organic impurities. Meanwhile, an industrial crystallization process is usually carried out in the metastable region to obtain high purity and high-quality products [18,19]. Moreover, the presence of organic impurities will also affect the metastable zone, seriously affecting the quality of products obtained in the crystallization process from actual wastewater [20]. However, less attention has been paid to this part of the data, so we focus more on this here.

Coal-to-liquids has prospered in Northwestern China. Both the water demand and wastewater generated is enormous. The accumulation of salts after evaporation and crystallization has seriously restricted local economic development. Therefore, based on Lu et al.'s [16] study on the relevant stable phase equilibrium in coal gasification wastewater, this study further studied the stability and metastable equilibrium phase diagram of the ternary system (NaCl + Na_2SO_4 + H_2O) in coal-to-liquids wastewater. At the same time, it was found that when wastewater is discharged into an evaporation pond or crystallizer, the temperature of the wastewater can be maintained at approximately 323.15 K. Therefore, we chose 323.15 K as the experimental temperature. By understanding the influence of organic impurities on the metastable zone, one can provide theoretical support for the actual local wastewater crystallization, and provide a reference for the crystallization of other coal-to-liquids wastewater.

2. Methodology

2.1. Materials and instruments

For measuring the phase equilibria, NaCl (AR, 99.5%), Na_2SO_4 (AR, 99.0%), $AgNO_3$ (AR, 99.8%), K_2SO_4 (AR, 99.0%), $BaCl{\cdot}2H_2O$ (AR, 99.5%) were all purchased from Sinopharm Chemical Reagent Co., Ltd., China. The wastewater was provided by a coal chemical industry company in the northwest of China. A comprehensive analysis of this wastewater was conducted, which showed that the wastewater was composed of 13 inorganic ions and 41 organic compositions. The main parameters are listed in Table 1. Doubly deionized water (electrical conductivity ≤ 10^{-4} S m^{-1}) was used for chemical analysis.

A THA-82 type constant temperature bath oscillator (Changzhou Runhua Electric Appliance Co., Ltd., China) with a temperature accuracy of ±0.05 K and temperature range of 293.15–373.15 K was used to achieve phase equilibration.

A set of jacketed glass evaporating crystallizers (Zhengzhou Greatwall Scientific Industrial and Trade Co., Ltd., China) was used for isothermal evaporation.

A ZDJ-58-D-type automatic titrator (Shanghai INESA Scientific Instrument Co., Ltd., China) was used to determine the solubility of NaCl and Na_2SO_4 in chemical analysis.

2.2. Experimental methods

The solubility of the ternary system Na^+/Cl^-, SO_4^{2-}–H_2O in coal-to-liquids wastewater was measured by using the isothermal solution saturation method [21]. The first salt was added into the wastewater forming a binary saturated solution in 250 mL flasks. The second salt was added into the binary saturation at 323.15 K [22] to obtain the saturated solution of the ternary system. The flasks were sealed and placed into a constant temperature bath oscillator for a certain period of time to accelerate the establishment of the balance. To ensure that the system was balanced, several samples of the system at 323.15 K were analyzed for Na^+, Cl^- and SO_4^{2-} after shaking for 4, 6, 8, and 10 h, separately. The experimental results showed that the concentration of Na^+, Cl^-, and SO_4^{2-} in the wastewater remained unchanged after 10 h. For the sake of caution, 12 h was selected to ensure solubility equilibrium. The oscillator was allowed to stand for 5 h to settle any remaining solids [23]. Then, the saturated solution was separated and moved into a 50 mL beaker to determine the solubility of Na_2SO_4 and NaCl.

Table 1
Water quality analysis of coal-to-liquids wastewater

No.	Parameter	Concentration[a]
1	Na^+	1,179.9 mol/kg
2	Cl^-	1,028.05 mol/kg
3	SO_4^{2-}	5,802.63 mol/kg
4	NO_3^-	130.22 mol/kg
5	K^+	19.55 mol/kg
6	F^-	1.71 mol/kg
7	HCO_3^-	97.60 mol/kg
8	pH	8.5
9	Chemical oxygen demand (COD)	279 mg/L
10	Biochemical oxygen demand (BOD_5)	698 mg/L
11	Total organic carbon (TOC)	1,039 mg/L

[a]Standard uncertainties u are $u(Cl^-)$ = 0.003; $u(Na^+)$ = 0.05; $u(SO_4^{2-})$ = 0.005; $u(NO_3^-)$ = 0.006; $u(K^+)$ = 0.03; $u(F^-)$ = 0.05; $u(HCO_3^-)$ = 0.02; u(pH) = 0.05; u(COD) = 0.5; $u(BOD_5)$ = 0.5; u(TOC) = 0.5.

Based on the solubility data, 1.5 L of the solution with a certain composition on the solubility curve was prepared by the isothermal solution saturation method in coal-to-liquids wastewater. When the system reached equilibrium, the saturated solution was moved into the jacketed glass evaporating crystallizer for isothermal evaporation. By adjusting the evaporator temperature, the evaporation temperature was maintained at 323.15 K. Then, six or more solid–liquid mixture samples (20 mL for each sample), which around the occurring point of the primary nucleation and the following points of further evaporation [24,25], were taken through the bottom valve. The solubility was determined by using a method based on measuring the solubility.

2.3. Analysis

The samples for the liquid phase and wet residues were added into pure doubly deionized water or a mixture of pure doubly deionized water and anhydrous ethanol (1:1 volume ratio). Then, the concentration of NaCl or Na_2SO_4 was determined by potentiometric precipitation titration [14] or metric titration with silver nitrate or barium chloride, respectively. The average relative error was less than ±0.003 or ±0.005, respectively. The density (ρ) was measured with a specific weighing bottle method with an uncertainty of ±0.001 [26]. The viscosity (η) was determined by an Ubbelohde Capillary Viscometer. An Abbe refractometer (WAY-2S) was used to measure the refractive index (n_D) with an uncertainty of 0.0002 [27]. A FE20 type pH meter (Shanghai Mettler Toledo Instruments Co., Ltd.) was used to determine the acidity and alkalinity of the solution [27].

2.4. Diagram presentation

When the concentration for the system is expressed as a dry salt mole percentage [23], it can be calculated by using Eq. (1).

$$J_i = \frac{m_i}{\left(m_{\mathrm{Cl}} + m_{\mathrm{S}}\right)} \times 100 \quad (1)$$

where i = 1, 2, and 3 express NaCl, Na_2SO_4, and H_2O, respectively. Cl and S denote NaCl and Na_2SO_4. m is the mole concentration for each molecular-based component. The phase diagram is presented by a rectangular coordinates diagram, where the X-axis is J_{NS} and the Y-axis is $J_{\mathrm{H_2O}}$.

3. Results and discussion

To verify the measurements, the solubility data for the stable phase equilibria for the ternary system (NaCl + Na_2SO_4 + H_2O) in pure water were obtained in this work, as shown in Table 2. At the same time, the conversion of experimental data to the Jänecke index is also listed in Table 2. The experimental data and the literature data [16] are plotted and shown in Fig. 1, respectively. As seen from Fig. 1, through comparison, it was found that the experimental data were highly consistent with the literature data, indicating that the experimental methods and equipment used in this work could be used to obtain reliable data and that the obtained data had high reliability in this work.

3.2. Stable phase diagrams for the ternary system (NaCl + Na_2SO_4 + H_2O) in coal-to-liquids wastewater

The phase equilibria experimental data for the solubility of the (NaCl + Na_2SO_4 + H_2O) system at 323.15 K are shown in Table 3; the conversion of the experimental data to the Jänecke index is also listed in Table 3. The relevant physical properties (n_D, η, ρ, and pH) are shown in Table 4. According to the experimental data, the corresponding phase diagram for the ternary system is shown in Fig. 2.

It can be seen from Fig. 2 that the stable phase diagram included one invariant point, two univariant curves, and three crystallization regions. Points A and C represent the saturation points for the binary systems (NaCl–H_2O) and (Na_2SO_4–H_2O) at 323.15 K in coal-to-liquids wastewater. Point E is the invariant point of the (NaCl + Na_2SO_4 + H_2O) system, which means that NaCl and Na_2SO_4 coexist in solution. The composition of the corresponding equilibrium solution was w (Na_2SO_4) = 5.35%, w (NaCl) = 23.74%. The

Table 2
Solid–liquid equilibrium and physical properties of saturated solutions of the ternary system (NaCl + Na_2SO_4 + H_2O) in pure water at 323.15 K and P = 88.4 kPa[a]

No.	Liquid composition (mass fraction, %)			Liquid composition (J/mol (100 mol dry salt)$^{-1}$)			Physical properties of liquid phase			
	NaCl	Na_2SO_4	H_2O	NaCl	Na_2SO_4	H_2O	ρ/(g cm^{-3})	η/10^{-3} Pa s^{-1}	n_D	pH
1, A^b	26.90	0.00	73.10	100.00	0.00	1,763.41	1.1850	1.1789	1.3770	7.20
2	26.24	0.88	71.35	97.31	2.69	1,716.80	1.1932	1.2022	1.3772	7.16
3, E^b	24.38	4.33	70.50	87.24	12.76	1,637.11	1.2145	1.2915	1.3781	7.02
4	18.41	9.11	72.10	71.05	28.95	1,805.89	1.2182	1.2835	1.3769	7.07
5	14.80	12.64	72.50	58.72	41.28	1,866.31	1.2210	1.3231	1.3756	7.11
6	12.63	15.54	71.55	49.68	50.32	1,826.27	1.2303	1.3545	1.3760	7.14
7	7.42	21.93	69.95	29.13	70.87	1,781.77	1.2516	1.4386	1.3761	7.19
8	3.59	26.81	69.60	13.99	86.01	1,760.01	1.2752	1.5671	1.3763	7.22
9, C^b	0.00	31.80	68.20	0.00	100.00	1,690.49	1.3040	1.8172	1.3769	7.26

[a]Standard uncertainties u are $u(T)$ = 0.05 K; $u(P)$ = 0.5 kPa; u(NaCl) = 0.003; u(Na_2SO_4) = 0.005; $u(n_D)$ = 0.0002; u(η) = 0.05; u(ρ) = 0.001; u(pH) = 0.01.
[b]Points: A, NaCl; E, (NaCl + Na_2SO_4); C, Na_2SO_4.

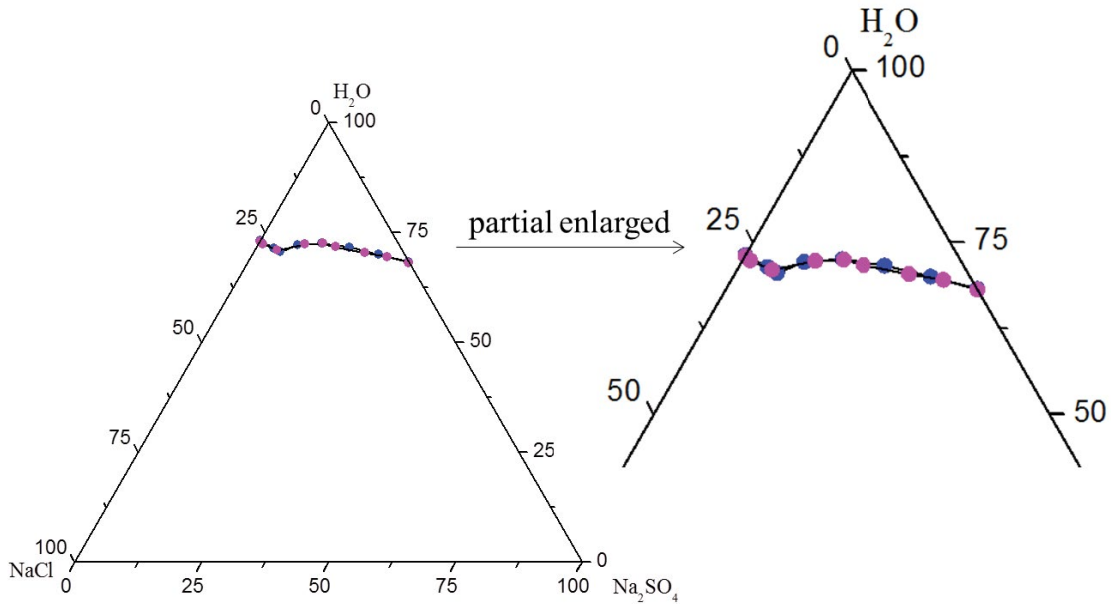

Fig. 1. Phase diagram for (NaCl + Na_2SO_4 + H_2O) in pure water at 323.15 K and P = 88.4 kPa. (●) experimental data; (●) literature data.

Table 3
Solid–liquid equilibrium of saturated solutions of the ternary system (NaCl + Na_2SO_4 + H_2O) in coal-to-liquids wastewater at 323.15 K and P = 88.4 kPa[a]

No.	Composition of the liquid phase, 100w		Composition of wet residue, 100w		Liquid composition (J/mol (100 mol dry salt)$^{-1}$)			Equilibrium solid phase[b]
	Na_2SO_4	NaCl	Na_2SO_4	NaCl	J_{NS}	J_{NC}	J_{H_2O}	
1, A[c]	4.01	24.29	0.01	84.35	11.96	88.04	1,681.60	Cl
2	4.81	24.12	1.21	61.82	14.10	85.90	1,636.85	Cl
3, E[c]	5.35	23.74	10.46	59.27	15.65	84.35	1,628.72	Cl + S
4	5.59	22.86	15.83	20.04	16.76	83.24	1,684.08	S
5	6.99	19.65	27.26	15.42	22.65	77.35	1,864.91	S
6	11.01	15.33	33.57	11.57	37.16	62.84	1,944.56	S
7	15.53	11.38	42.33	7.46	52.91	47.09	1,941.50	S
8	20.60	7.28	55.05	3.62	69.97	30.03	1,902.92	S
9, C[c]	25.53	3.12	64.25	1.58	87.07	12.93	1,883.49	S

[a]Standard uncertainties u are $u(T)$ = 0.05 K; $u(P)$ = 0.5 kPa; u(NaCl) = 0.003; $u(Na_2SO_4)$ = 0.005.
[b]Cl: NaCl; S: Na_2SO_4.
[c]Points: A, NaCl; E, (NaCl + Na_2SO_4); C, Na_2SO_4.

curve AE shows that NaCl is saturated in the wastewater, where NaCl is precipitated. However, along with the curve CE, Na_2SO_4 shows priority to precipitate. In addition, IV is the unsaturated solution region of NaCl and Na_2SO_4, in which no salt will reach saturation and crystallize out from the solution. Three crystallization fields are corresponding to I (NaCl), II (Na_2SO_4), and III (NaCl + Na_2SO_4) in coal-to-liquids. The crystallization region of Na_2SO_4 is greater than that of NaCl and the solubility of Na_2SO_4 always increases with decreasing NaCl concentration at 323.15 K. As shown in Eq. (2), the concentration of Na^+ will increase due to the dissolution of Na_2SO_4 in the saturated NaCl solution. As a result of the ion effect, the dissolution equilibrium in Eq. (3) moves to the left and leads to a decrease in the solubility of NaCl. The larger crystallization region means that the solubility of Na_2SO_4 in the (NaCl + Na_2SO_4 + H_2O) system in wastewater is low and Na_2SO_4 will salt out of the solution easily with increasing NaCl concentration. A double salt or solid solution was not discovered in this system at 323.15 K. Furthermore, the components of the equilibrium solid phases were further studied by X-ray diffraction (XRD). The XRD pattern in Fig. 3 shows that point E is the ternary co-saturation point of Na_2SO_4 and NaCl in this system. The experimental results from XRD characterization are consistent with Schreinemaker's method [26], which also proves the above conclusions:

Table 4
Physical properties of saturated solutions of the ternary system (NaCl + Na_2SO_4 + H_2O) in coal-to-liquids wastewater at 323.15 K and P = 88.4 kPa[a]

No.	Physical properties of liquid phase			
	ρ/(g cm^{-3})	η/10^{-3} Pa s^{-1}	n_D	pH
1, A[b]	1.2285	1.3105	1.3801	7.67
2	1.2288	1.3137	1.3810	7.61
3, E[b]	1.2331	1.3197	1.3813	7.58
4	1.2301	1.3160	1.3803	7.61
5	1.2204	1.2921	1.3789	7.72
6	1.2275	1.3179	1.3758	7.80
7	1.2427	1.4007	1.3745	7.88
8	1.2654	1.4340	1.3740	7.97
9, C[b]	1.2826	1.6152	1.3746	8.04

[a]Standard uncertainties u are $u(T)$ = 0.05 K; $u(P)$ = 0.5 kPa; $u(n_D)$ = 0.0002; u(η) = 0.05, u(ρ) = 0.001; u(pH) = 0.01.
[b]Points: A, NaCl; E, (NaCl + Na_2SO_4); C, Na_2SO_4.

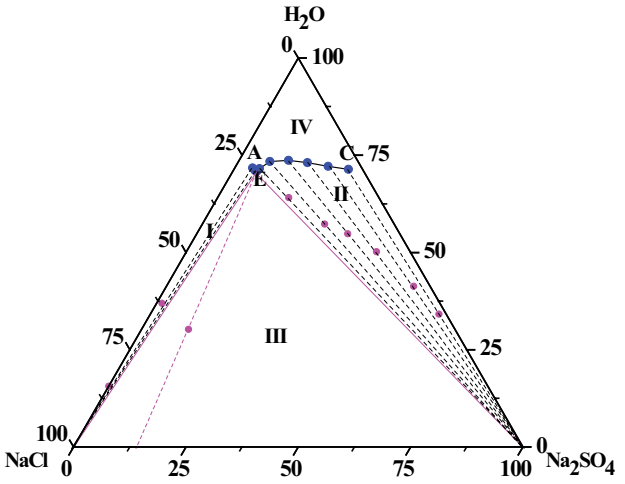

Fig. 2. Phase diagram for (NaCl + Na_2SO_4 + H_2O) in coal-to-liquids wastewater at 323.15 K and P = 88.4 kPa. (●) Equilibrium liquid phase composition; (●) moist solid phase composition; A, the solubility of NaCl in coal-to-liquid wastewater at 323.15 K; C, the solubility of Na_2SO_4 in coal-to-liquid wastewater at 323.15 K; E, invariant point of NaCl and Na_2SO_4 in coal-to-liquid wastewater.

$$Na_2SO_4(s) \rightarrow 2Na^+(aq) + SO_4^{2-}(aq) \quad (2)$$

$$NaCl(s) \rightarrow Na^+(aq) + Cl^-(aq) \quad (3)$$

In addition, Fig. 4 indicates the relationship between the physical properties (ρ, η, n_D, and pH) and the mass fraction of Na_2SO_4 in the wastewater. As the concentration of Na_2SO_4 increases, the physical properties also change. All E points were obvious turning points. With increasing Na_2SO_4 concentration, the viscosity and density values show a similar trend to increase, but the refractive index and pH values show different behaviors. The refractive index increased

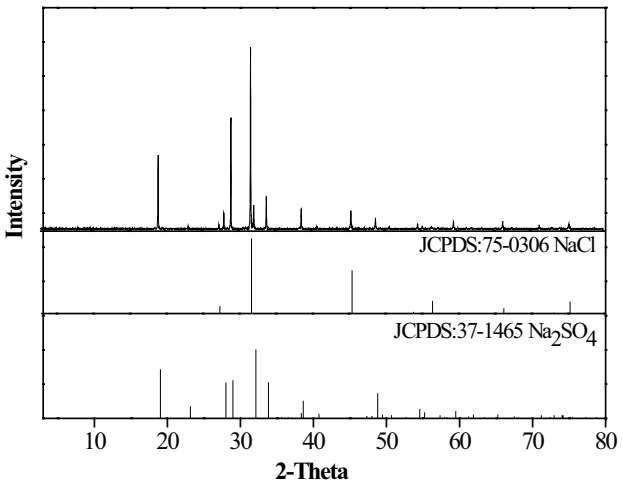

Fig. 3. XRD pattern of the invariant point E of the ternary system Na^+//Cl^-, SO_4^{2-}–H_2O in coal-to-liquids wastewater at 323.15 K.

first and then decreased with increasing w (Na_2SO_4), but the pH values decreased first and then increased with increasing w (Na_2SO_4). This means that different physical properties will change with the increase in Na_2SO_4 and show different rules.

3.3. Metastable phase diagrams for the ternary system (NaCl + Na_2SO_4 + H_2O) in coal-to-liquids wastewater

The metastable zone refers to the distance between the super solubility curve and the solubility curve of the system. In the process operation, it is necessary to control the operation in the stable zone to prevent deterioration of the crystallization product, so the metastable zone has important guiding significance for the actual production operation. The saturated solution for different points in pure water and coal-to-liquids wastewater was evaporated at 323.15 K, respectively. The solutions of 1–9 illustrated in Tables 2 and 3 were boiled to evaporate at 323.15 K with an evaporation rate of 3.8 g (d cm^2)$^{-1}$ (water). The primary points and the width of the metastable zones are displayed in Table 5, and the metastable phase diagrams are shown in Fig. 5.

When comparing the metastable phase diagrams for the (NaCl + Na_2SO_4 + H_2O) system in pure water and coal-to-liquids wastewater, as shown in Fig. 5, the metastable curve of the NaCl-rich side shows little change, besides that of the Na_2SO_4-rich side shifting slightly downwards, and the co-saturated point obviously shifting left in coal-to-liquids wastewater. This demonstrated that the impurities in the wastewater had an effect on the crystallization of NaCl and Na_2SO_4 and that the effect on Na_2SO_4 was more significant. In other words, the nucleation rate and crystal growth of Na_2SO_4 were slowed down compared to NaCl, and the driving force required for nucleation was significantly increased in coal-to-liquids wastewater [28].

3.4. Phase diagram comparison

As shown in Fig. 6, a similar trend was obtained for the solubility of the (NaCl + Na_2SO_4 + H_2O) system in pure

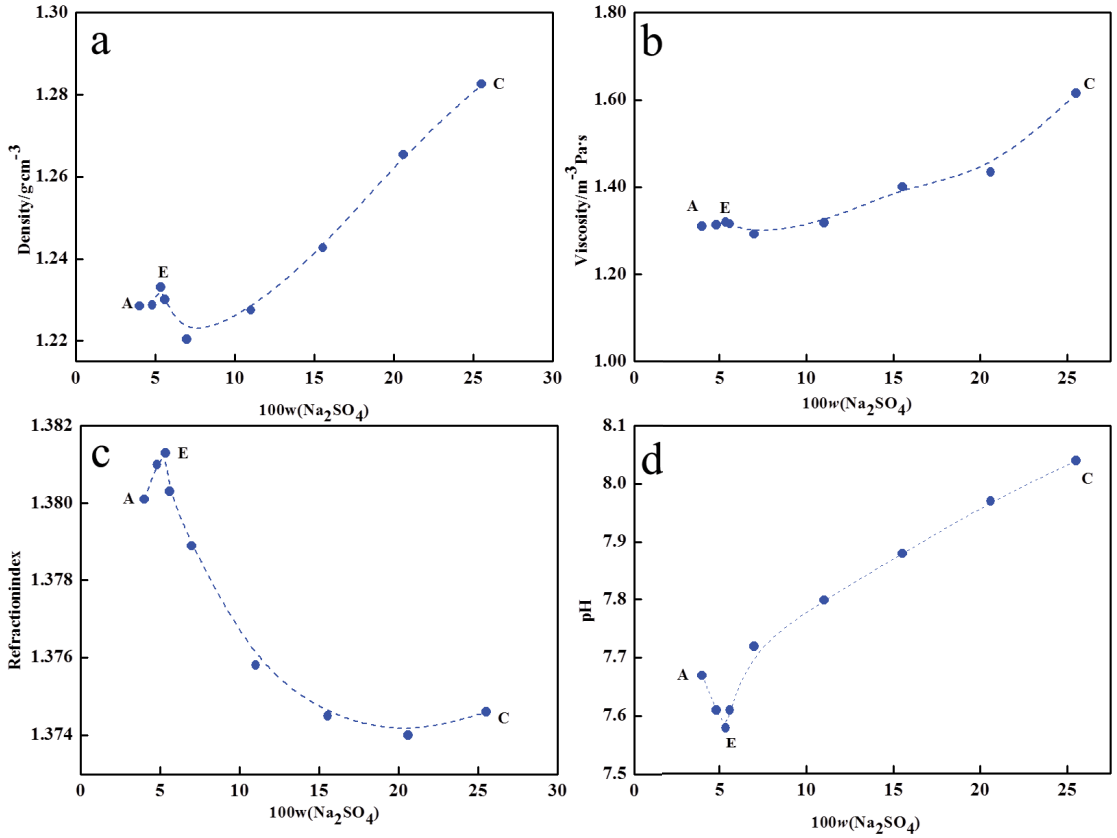

Fig. 4. Physical properties vs. w (Na_2SO_4) of (NaCl + Na_2SO_4 + H_2O) in coal-to-liquids wastewater at 323.15 K and P = 88.4 kPa. (a) Density values w (Na_2SO_4), (b) viscosity vs. w (Na_2SO_4), (c) refractive index vs. w (Na_2SO_4), and (d) pH vs. w (Na_2SO_4).

water, coal-to-liquids wastewater, and literature at 323.15 K. AE and CE are the solubility curves of NaCl and Na_2SO_4, respectively. It is worth noting that because coal-to-liquids wastewater already contains NaCl and Na_2SO_4, AE and CE will not intersect with BW and DW in coal-to-liquids wastewater, respectively. Apparently, the crystallization region of Na_2SO_4 in coal-to-liquids wastewater was larger than that in pure water, but the crystallization region of NaCl shows no significant change in coal-to-liquids wastewater and pure water. Furthermore, the solubility curve of Na_2SO_4 in coal-to-liquids wastewater is obviously higher than that in pure water at 323.15 K, revealing that the solubility of Na_2SO_4 grows lower in coal-to-liquids wastewater than that in pure water at 323.15 K. Su et al. [17] and Becheleni et al. [29] also found that the presence of phenol has a significant effect on the solubility of Na_2SO_4, which reduces the solubility of Na_2SO_4 in water. However, the results of this work are exactly the opposite of those obtained by Lu et al. [16] in coal gasification wastewater at 323.15 K. In the study of Lu et al. [16], the solubility of Na_2SO_4 in coal gasification wastewater was higher than that in pure water at 323.15 K, and the solubility of NaCl did not change much. This indicates that the solubility of Na_2SO_4 in wastewater produced in different process stages is not the same. Therefore, all the results can prove that the presence of impurities in wastewater has a greater impact on the solubility of Na_2SO_4 and less on NaCl.

The stable and metastable phase diagrams for the system in pure water and coal-to-liquids wastewater at 323.15 K and 88.4 kPa are shown in Figs. 7 and 8, respectively. The salt-forming region is mainly determined by thermodynamic conditions and is a region where salt can be formed by primary nucleation or crystal growth. Primary nucleation is further divided into homogeneous nucleation or heterogeneous nucleation according to the difference between a spontaneous process and foreign particle catalysis. In this work, primary nucleation is homogeneous nucleation because no foreign particles are added. At this time, the primary region (PR) is where the homogeneous nucleation of the considered salt can arise during isothermal concentration.

As shown in Figs. 7 and 8, the solubility region (SR) is an area in which the solution is equilibrated. O and O* are the co-saturated and co-nucleation points of the stable and metastable equilibria phase diagrams, respectively. The projection points for O, O* parallel to the water-free edge, indicate the widths of the solubility region SR_{NC}, SR_{NS}, and primary region PR_{NC}, PR_{NS}, respectively. Due to the SR and PR boundary relationship, the phase law also applies to the primary region where $SR_{NC} + SR_{NS} = 1$, $PR_{NC} + PR_{NS} = 1$ [23]. As shown in Fig. 7, O, and O* deviate from each other, resulting in $SR_{NC} < PR_{NC.}$ Similarly, a similar phenomenon is observed in Fig. 7, but the deviation between O and O* is relatively small.

The region between the solubility and the super solubility curve is defined as the metastable region. A certain driving

Table 5
Metastable equilibrium of the ternary system (NaCl + Na_2SO_4 + H_2O) in pure water and coal-to-liquids wastewater at 323.15 K and P = 88.4 kPa[a]

System	No.	Composition of liquid phase, 100w		Composition of wet residue, 100w		Liquid composition (J/mol (100 mol dry salt)$^{-1}$)			Metastable zone (J/mol (100 mol dry salt)$^{-1}$)	Equilibrium solid phase[b]
		Na_2SO_4	NaCl	Na_2SO_4	NaCl	J_{NC}	J_{NS}	J_{H_2O}		
In pure water	1	0.00	27.48	ND[d]	ND[d]	100	0.00	1,736.58	26.83	Cl
	2	1.52	26.87	1.01	65.50	95.55	4.45	1,675.28	41.52	Cl
	3	6.16	23.59	26.20	37.08	82.31	17.69	1,590.52	46.59	Cl + S
	4	8.50	21.47	18.03	19.46	75.42	24.58	1,596.32	209.56	S
	5	12.30	17.64	23.71	15.45	63.53	36.47	1,637.36	228.95	S
	6	15.79	14.74	30.29	12.06	53.14	46.86	1,625.14	201.12	S
	7	20.06	10.70	36.19	8.66	39.32	60.68	1,650.99	130.78	S
	8	24.32	6.73	49.12	4.33	25.16	74.84	1,672.53	87.49	S
	9	33.45	0.00	ND[d]	ND[d]	0.00	100.00	1,568.28	122.20	S
In CTLW[c]	1	4.84	24.81	ND[d]	ND[d]	86.16	13.84	1,573.47	108.13	Cl
	2	5.37	24.45	2.82	52.21	84.69	15.31	1,566.38	70.47	Cl
	3	5.55	24.05	24.49	24.88	84.03	15.97	1,605.56	23.16	Cl + S
	4	6.36	23.88	35.76	16.43	82.02	17.98	1,572.82	111.26	S
	5	7.32	22.72	40.35	14.44	79.04	20.96	1,579.27	285.64	S
	6	8.27	22.25	46.78	12.76	76.57	23.43	1,551.59	392.97	S
	7	12.69	18.75	49.54	10.48	64.22	35.78	1,557.55	383.95	S
	8	18.93	12.42	52.18	6.95	44.35	55.65	1,603.97	298.95	S
	9	25.60	6.93	ND[d]	ND[d]	24.75	75.25	1,563.36	320.13	S

[a]Standard uncertainties u are $u(T)$ = 0.05 K; $u(P)$ = 0.5 kPa; u(NaCl) = 0.003, $u(Na_2SO_4)$ = 0.005.
[b]Cl: NaCl; S: Na_2SO_4.
[c]CTLW: coal-to-liquids wastewater.
[d]ND: not determined.

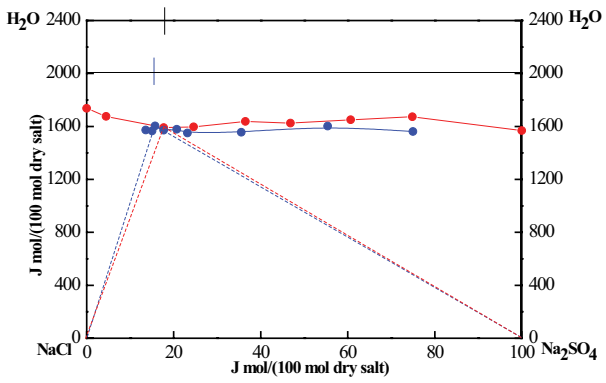

Fig. 5. Comparison of the metastable equilibrium phase diagrams of (NaCl + Na_2SO_4 + H_2O) system in pure water and coal-to-liquids wastewater at 323.15 K and P = 88.4 kPa. (●) in pure water; (●) in coal-to-liquids wastewater.

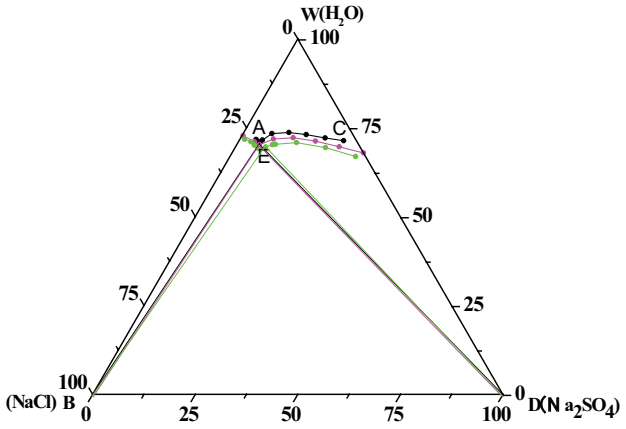

Fig. 6. Phase diagram for (NaCl + Na_2SO_4 + H_2O) in coal-to-liquids wastewater and pure water at 323.15 K and P = 88.4 kPa. (●) in coal-to-liquids wastewater; (●) in pure water; (●) in coal gasification wastewater from literature. A, the solubility of NaCl in coal-to-liquids wastewater at 323.15 K; C, the solubility of Na_2SO_4 in coal-to-liquids wastewater at 323.15 K; E, invariant point of NaCl and Na_2SO_4 in coal-to-liquids wastewater; B, pure solid of NaCl; D, pure solid of Na_2SO_4; W, H_2O.

force is needed during the salt formation process to help it nucleate as quickly as possible. However, different salts have different metastable zone widths (MSZW), which means that nucleation of different salts requires different driving forces, leading to deviations between the salt-forming region and the solubility region.

The average MSZW is the average value of all the MSZW corresponding to the test point with the same equilibrium solid phase in a system and can be calculated by using Eq. (4).

$$A_s = \frac{(\Sigma W_i)}{n} \tag{4}$$

where A stands for the average MSZW value, s stands for the equilibrium solid phase, W expresses the MSZW

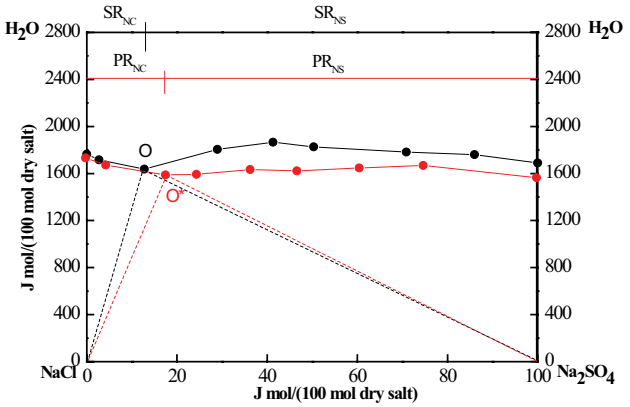

Fig. 7. Comparison of the stable and metastable equilibrium phase diagrams of (NaCl + Na_2SO_4 + H_2O) system in pure water at 323.15 K and P = 88.4 kPa. (●) stable equilibrium phase diagrams; (●) metastable equilibrium phase diagrams.

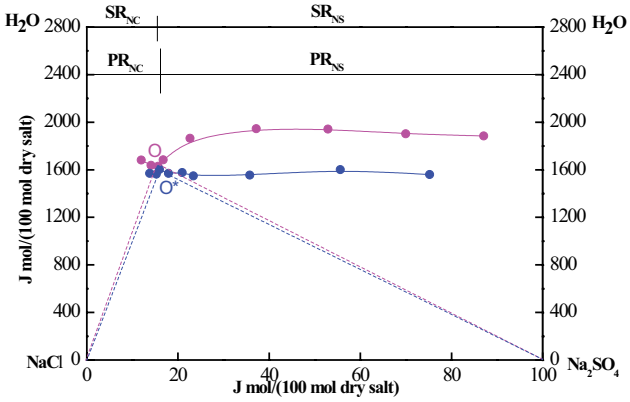

Fig. 8. Comparison of the stable and metastable equilibrium phase diagrams of (NaCl + Na_2SO_4 + H_2O) system in coal-to-liquids wastewater at 323.15 K and P = 88.4 kPa. (●) stable equilibrium phase diagrams; (●) metastable equilibrium phase diagrams.

value of the test point i, n represents the number of test points with the same equilibrium solid phase.

The average MSZW for the ternary system in pure water and coal-to-liquids wastewater is listed in Table 6. As shown in Table 6, comparing the average MSZW of Na_2SO_4 in pure water and coal-to-liquids wastewater, the average MSZW of Na_2SO_4 was significantly broadened in the coal-to-liquids wastewater. The average MSZW of Na_2SO_4 increased by approximately 76.89%, revealing an increase in the nucleation driving force of Na_2SO_4. That is, the nucleation rate and crystal growth of Na_2SO_4 were slowed down, which is not conducive to the crystallization of Na_2SO_4. This may be due to the presence of some organic impurities in the wastewater, which affects the properties of Na_2SO_4 in water. At the same time, the average MSZW change in the NaCl-rich side was slightly widened, indicating that the presence of organic impurities in the wastewater had little effect on the nucleation driving force of NaCl. Therefore,

Table 6
Average MSZW[a] of the ternary system (NaCl + Na_2SO_4 + H_2O) in pure water and coal-to-liquids wastewater at 323.15 K and P = 88.4 kPa[b]

Solid	System	Average MSZW (J_{H_2O}/mol (100 mol dry salt)$^{-1}$)
NaCl	In pure water	38.31
	In CTLW[c]	67.25
Na_2SO_4	In pure water	146.67
	In CTLW	259.44

[a]MSZW: metastable zone width.
[b]Standard uncertainties u are $u(T)$ = 0.05 K; $u(P)$ = 0.5 kPa.
[c]CTLW: coal-to-liquids wastewater.

organic impurities in the wastewater were strictly controlled during the evaporation crystallization process to ensure that high-quality salts were obtained with a small driving force.

4. Conclusion

The ternary system of (NaCl + Na_2SO_4 + H_2O) in coal-to-liquids wastewater was studied at 323.15 K. According to experimental results, the stable and metastable phase diagrams for coal-to-liquids wastewater were investigated and compared with those for pure water. It was found that the NaCl-rich side showed little change, besides that of the Na_2SO_4-rich side in the stable and metastable phase diagrams. In stable phase diagrams, the Na_2SO_4-rich side was found to be lower in coal-to-liquids wastewater than in pure water. In metastable phase diagrams, the Na_2SO_4-rich side shifted slightly downwards in coal-to-liquids wastewater, and the co-nucleation points obviously shifted left in the metastable phase diagrams. The average MSZW is significantly enlarged in the Na_2SO_4-rich side, increasing by approximately 76.89%. Organic impurities in wastewater have a significant effect on Na_2SO_4, which leads to a decrease in the solubility of Na_2SO_4 and an increase in the crystalline region. The nucleation driving force for Na_2SO_4 was greatly affected, which caused the nucleation rate and crystal growth rate for Na_2SO_4 to slow down. All results obtained in this experiment can be used for the desalination process for NaCl and Na_2SO_4 in industrial production and further theoretical studies.

Acknowledgment

This research was financially supported by The East-West Cooperation Project of Ningxia Key R & D Plan (2017BY064), and National First-rate Discipline Construction Project of Ningxia (NXYLXK2017A04).

Symbols

XRD	—	X-ray powder diffraction
CTLW	—	Coal-to-liquids wastewater
n_D	—	Solution refractive index
η	—	Solution viscosity
ρ	—	Solution density
J	—	Dry salt mole percentage
m	—	Mole concentration for each molecular based component
$u(T)$	—	Standard uncertainty of temperature
$u(P)$	—	Standard uncertainty of pressure
$u(n_D)$	—	Standard uncertainty of refractive index
u(η)	—	Standard uncertainty of viscosity
u(ρ)	—	Standard uncertainty of density
u(pH)	—	Standard uncertainty of pH
PR	—	Primary region
SR	—	Solubility region
MSZW	—	Metastable zone width
A	—	Average metastable zone width

References

[1] P. Badiuzzaman, E. Mclaughlin, D. McCauley, Substituting freshwater: can ocean desalination and water recycling capacities substitute for groundwater depletion in California?, J. Environ. Manage., 203 (2017) 123–135.
[2] K.L. Timofeev, A.B. Lebed, A.J. Malyutin, Deep treatment of copper plant waste water streams with water recycling, Solid State Phenom., 265 (2017) 937–944.
[3] H. Mirbolooki, R. Amirnezhad, A.P. Pendashteh, Treatment of high saline textile wastewater by activated sludge microorganisms, J. Appl. Res. Technol., 15 (2017) 167–172.
[4] A. Garg, Wet oxidation: a promising option for the treatment of pulp and paper mill wastewater, J. Inst. Eng. (India): Ser. A., 93 (2012) 137–141.
[5] V. Manivannan, L. Elango, Leather processing and its possible impact on groundwater quality in Silk Road sites: a case study from Chennai, India, Environ. Earth Sci., 76 (2017) 44.
[6] J.P. Xu, S.H. Hou, H.P. Xie, C.W. Lv, L.M. Yao, Equilibrium approach towards water resource management and pollution control in coal chemical industrial park, J. Environ. Manage., 219 (2018) 56–73.
[7] P.Z. Cui, Z.H. Mai, S.Y. Yang, Y. Qian, Integrated treatment processes for coal-gasification wastewater with high concentration of phenol and ammonia, J. Cleaner Prod, 142 (2017) 2218–2226.
[8] B.L. Hou, H.J. Han, S.Y. Jia, H.F. Zhuang, Q. Zhao, P. Xu, Effect of alkalinity on nitrite accumulation in treatment of coal chemical industry wastewater using moving bed biofilm reactor, J. Environ. Sci. China, 26 (2014) 1014–1022.
[9] O. Lefebvre, R. Moletta, Treatment of organic pollution in industrial saline wastewater: a literature review, Water Res., 40 (2006) 3671–3682.
[10] H. Zhu, Y.X. Han, C.Y. Xu, H.J. Han, W.W. Ma, Overview of the state of the art of processes and technical bottlenecks for coal gasification wastewater treatment, Sci. Total Environ., 637–638 (2018) 1108–1126.
[11] C.F. Yang, Y. Qian, L.J. Zhang, J.Z. Feng, Solvent extraction process development and on-site trial-plant for phenol removal from industrial coal-gasification wastewater, Chem. Eng. J., 117 (2006) 179–185.
[12] M. Ahmed, W.H. Shayya, D. Hoey, A. Mahendran, R. Morris, J. Al-Handaly, Use of evaporation ponds for brine disposal in desalination plants, Desalination, 130 (2000) 155–168.
[13] P.Z. Cui, Y. Qian, S.Y. Yang, New water treatment index system toward zero liquid discharge for sustainable coal chemical processes, ACS Sustainable Chem. Eng., 6 (2018) 1370–1378.
[14] X.R. Zhang, Y.S. Ren, P. Li, H.J. Ma, W.J. Ma, C.Q. Liu, Y.N. Wang, L.X. Kong, W. Shen, Solid–liquid equilibrium for the ternary systems (Na_2SO_4 + NaH_2PO_4 + H_2O) and (Na_2SO_4 + NaCl + H_2O) at 313.15 K and atmospheric pressure, J. Chem. Eng. Data, 59 (2014) 3969–3974.
[15] C. Bian, H. Chen, X.F. Song, Y. Jin, J.G. Yu, Stable phase equilibria of the quaternary system Na^+//Cl^-, NO_3^-, SO_4^{2-}–H_2O at 353.15 K, J. Chem. Eng. Data, 63 (2018) 3305–3314.

[16] H.J. Lu, J.K. Wang, J. Yu, Y.F. Wu, T. Wang, Y. Bao, D. Ma, H.X. Hao, Phase equilibria for the pseudo-ternary system (NaCl + Na_2SO_4 + H_2O) of coal gasification wastewater at T = (268.15 to 373.15) K, Chin. J. Chem. Eng., 25 (2017) 955–962.
[17] N.N. Su, Y.L. Wang, Y. Xiao, H.J. Lu, Y.J. Lou, J.J. Huang, M. He, Y. Li, H.X. Hao, Mechanism of influence of organic impurity on crystallization of sodium sulfate, Ind. Eng. Chem. Res., 57 (2018) 1705–1713.
[18] J.Y. Peng, Y.P. Dong, L.P. Wang, L.L. Li, W. Li, H.T. Feng, Effect of impurities on the solubility, metastable zone width, and nucleation kinetics of borax decahydrate, Ind. Eng. Chem. Res., 53 (2014) 12170–12178.
[19] S. Gupta, L. Pel, M. Steiger, K. Kopinga, The effect of ferrocyanide ions on sodium chloride crystallization in salt mixtures, J. Cryst. Growth, 410 (2015) 7–13.
[20] K. Sangwal, On the effect of impurities on the metastable zone width of phosphoric acid, J. Cryst. Growth, 312 (2010) 3316–3325.
[21] T.T. He, J.J. Sun, W. Shen, Y.S. Ren, Solid-liquid phase equilibria of quaternary system NH_4^+//C1$^-$, SO_4^{2-}, $H_2PO_4^-$–H_2O and its subsystems NH_4^+//C1$^-$, SO_4^{2-}–H_2O, NH_4^+//C1$^-$, $H_2PO_4^-$–H_2O at 313.15 K, J. Chem. Thermodyn., 112 (2017) 31–42.
[22] J. Xie, X. Liu, W. Pan, C. Cai, Y.S. Ren, Phase equilibria in the system Na^+, K^+//SO_4^{2-}-$(CH_2OH)_2$-H_2O and Na^+, K^+//Cl^-, SO_4^{2-}-$(CH_2OH)_2$-H_2O at 328.15 K, J. Chem. Thermodyn., 112 (2017) 155–165.
[23] H. Zhou, Y.J. Bao, X.Q. Bai, R.X. Ma, L. Huangfu, C. Zhang, Salt-forming regions of seawater type solution in the evaporation and fractional crystallization process, Fluid Phase Equilib., 362 (2014) 281–287.
[24] H. Zhou, Y.D. Chen, Q.Y. Kang, J.B. Zhang, H.L. Zhang, J.J. Yuan, Z.L. Sha, Non-equilibrium state salt-forming phase diagram: utilization of bittern resource in high efficiency, Chin. J. Chem. Eng., 18 (2010) 635–641.
[25] W. Shen, Y.S. Ren, T. Wang, C. Hai, Stable (solid + liquid) phase equilibrium for the ternary systems (K_2SO_4 + KH_2PO_4 + H_2O), (K_2SO_4 + KCl + H_2O) at T = 313.15 K, J. Chem. Thermodyn., 90 (2015) 15–23.
[26] L.Z. Meng, T.L. Deng, Y.F. Guo, D. Li, L. Yang, Measurement and thermodynamic model study on solid + liquid equilibria and physicochemical properties of the ternary system $MgBr_2$ + $MgSO_4$ + H_2O at 323.15 K, Fluid Phase Equilib., 342 (2013) 88–94.
[27] J. Cao, Y.S. Ren, B.J. Yu, L.S. Qiu, F.Y. Ma, Solid-liquid equilibrium for the ternary systems (Na_2CO_3 + NaCl + H_2O) and (Na_2CO_3 + Na_2SO_4 + H_2O) at 313.15 K and atmospheric pressure, J. Chem. Thermodyn., 133 (2019) 181–193.
[28] H. Zhou, H.L. Zhang, Y.D. Chen, J.B. Zhang, S. Zhang, X.Q. Bai, Salt-forming regions of the Na^+, Mg^{2+}//Cl^-, SO4^{2-}–H_2O system at 348.15 K in the nonequilibrium state of isothermal boiling evaporation, J. Chem. Eng. Data, 57 (2012) 943–951.
[29] E.M.A. Becheleni, M. Rodriguez-Pascual, A.E. Lewis, S.D.F. Rocha, Influence of phenol on the crystallization kinetics and quality of ice and sodium sulfate decahydrate during eutectic freeze crystallization, Ind. Eng. Chem. Res., 56 (2017) 11926–11935.